

RADAR OBSERVATION OF INTENSE RAIN EVENTS DURING THE BOLLENE 2002 EXPERIMENT

John Nicol¹, Guy Delrieu¹, Dominique Faure² and Pierre Tabary³

¹L.T.H.E., Grenoble, France : nicol@hmg.inpg.fr

²Alicime, Lyon, France

³Météo France, Paris, France

Abstract

During the autumn 2002, an operational S-band radar employed by Météo France tested a volume sampling scanning protocol at Bollène, south-east France. This region often suffers intense and long-lasting precipitation and also poses problems for radar measurements due to the significant topography. The experiment is intended to study the benefit of a volume sampling strategy in this region and to study the local climatology. Processing procedures for data quality analysis and corrections are described and some examples are given. Radar rain estimates are compared to rain gauge measurements providing bias estimates used for recalibration and several other criteria for the evaluation of the radar rain estimates and the corresponding corrections. Observed vertical profiles of reflectivity show dramatic differences on an event-by-event basis, while the mean 'climatological' profile displays a gradient of approximately -3 dBZ/km in the lowest 5 km. Vertical profile correction and Z-R relationship variability are expected to be the dominant factors influencing measurement accuracy.

Key Words: Volume scanning radar, quantitative rainfall estimates, data quality control, rain gauge validation.

Introduction

The Bollène 2002 experiment was designed with Météo France with two primary goals; to test the benefit of a volume scanning strategy for both hydrological and meteorological applications of weather radar and to improve the understanding of systems which often lead to severe flooding, in this region. An S-band radar belonging to the operational French radar network (ARAMIS) was used for this purpose. Bollène is located in the Rhone Valley (south-east France) between two mountain ranges (the Massif Central and the foothills of the French Alps) approximately 120 km north of the Mediterranean Sea as shown in Figure 1. This region is prone to intense rain events which often occur within warm sectors of Mediterranean perturbations during autumn (Riverain 1998). These synoptic features lead to the advection of warm and humid air from the Mediterranean Sea towards coastal regions. The pronounced relief triggers convection and channels low-level flow inducing convergence contributing to the release of convective instability. Various precipitating systems may result ranging from orographic systems associated with shallow convection to meso-scale convective system associated with deep convection.

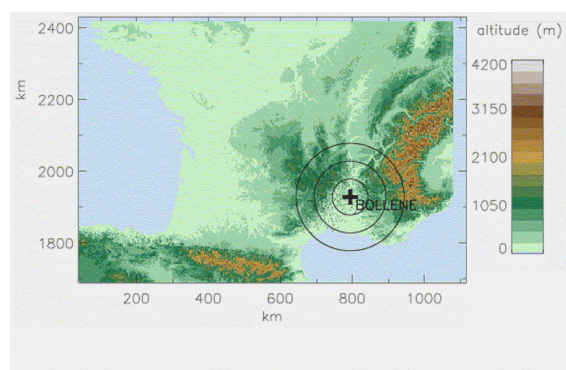


Figure 1: Location of the Bollène radar in south-east France, range rings are shown at 50 km intervals to 150 km.

The ARAMIS network has previously provided operational meteorological products, using a few low level elevation scans to form pseudo-CAPPIs (with lower elevations used at further range intervals). While

necessitating faster scans rates to obtain similar temporal resolution, a volume scanning protocol allows many advantages with respect to data quality. A dense network of rain gauges (365 gauges, $\sim 1/100 \text{ km}^2$) cover the chosen research region (the Cevéennes-Vivarais) as shown in Figure 2 and are used for calibration and evaluation purposes. Both 'static' and 'dynamic' data processing are developed for the estimation of rain rate fields at ground level with a view to the evaluation of the relative ability of the corrections. 'Static' approaches use 'information a priori' products such as dry weather ground clutter maps and climatological vertical profiles of reflectivity (VPR). 'Dynamic' approach uses adaptive treatments, utilising data on a scan-by-scan basis. These include; the identification of ground clutter areas using a combination of a variability criterion derived from the inter-pulse radar signal and of horizontal reflectivity gradients, and the use of ground clutter targets of high intensity and low variability (low SIGMA, hence clutter) to analyse radar calibration stability. The processing is based on a modular approach allowing the inclusion of various correction procedures to evaluate the relative improvement in terms of rainfall estimation.

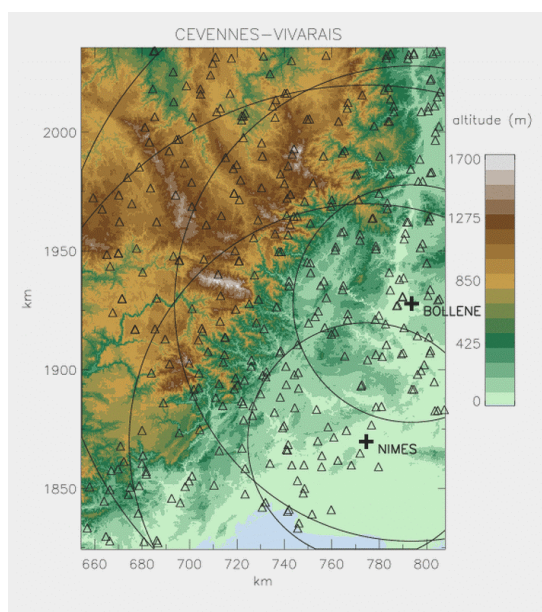


Figure 2: The topography of the Cevéennes-Vivarais region, showing the radar at Bollène and the sites of the 365 rain gauges (triangles) and the neighbouring radar at Nimés.

The rain gauge accumulations are used to create 2D rain and error estimates using interpolation based on krigage. Selected parts of rain fields derived from the radar and gauge network measurements are then compared for calculating biases in the accumulations and other similarity criteria. Only regions with low estimated standard deviation (eg normalised std. dev. $< 40\%$) in the kriged-rain gauge field and which are also outside regions of affected by ground clutter and beam shielding are used in the comparison. The analyses presently consider daily and event-long gauge accumulations. This will be complimented by hourly comparisons for which 170 gauges exist in the study region. Future work will focus on the correction of the vertical profile of reflectivity (VPR) and its association with Z-R relationships and drop size distributions.

Bollène 2002 experiment

Operating protocol and data set

Between September and December 2002, the radar at Bollène was operated with an "interlaced" volume scanning strategy: 8 PPIs were performed every 5 min. with antenna rotation speeds of $10^\circ/\text{s}$ (low elevation angles) and $15^\circ/\text{s}$ (higher elevation angles). 3 PPIs at elevation angles of 0.8° , 1.2° and 1.8° were repeated every 5 min. to provide the pre-existing operational products. Two sets of additional angles (0.4° , 3.6° , 6.0° , 9.0° , 14.0° and 2.4° , 4.8° , 7.3° , 11.1° , 18.0°) were alternated every 5 min. in order to optimise the volume sampling of atmosphere. Hence, a 'complete' volume scan was accomplished every 10 min. Both the average reflectivity (Z, stored as dBZ) and the inter-pulse variability (SIGMA) are archived for each PPI with a spatial resolution of 1 km^2 . SIGMA, which is the absolute difference in reflectivity (dBZ) between each second pulse, averaged over the Cartesian grid, is used as part of a ground clutter identification procedure both for the elimination and the identification of non-raining regions of intense clutter for calibration stability analysis. The autumn 2002 had about 21 rainy days in the Cevéennes-Vivarais region, of these several

produced significant accumulations near the Bollène radar, allowing accurate comparisons. The radar worked well with the new operating protocol during this period, providing a unique data set including the catastrophic 8-9th Sept. event in the Gard region in which rain accumulations over 600 mm were recorded in 24 hours by both radar and rain gauges.

Radar processing strategies and validation

The final objective of this project is to define optimal processing strategies to obtain both temporal 2D (ground level rain amounts) and eventually 3D (water content) hydro-meteorological products to be used for the forcing and/or validation of meteorological and hydrological models. Naturally, quality control is critical in any analysis and the current work is ongoing. A number of preliminary studies have and are being conducted on the following subjects; Ground clutter identification, beam shielding correction, vertical profile of reflectivity measurement and correction, precipitation type classification and calibration analysis. Some examples are given in the following sections.

Ground clutter

The ground clutter identification scheme uses a combination of the mean inter-pulse variability on a scan-by-scan basis and neighbouring horizontal reflectivity gradients. The product SIGMA for the Bollène radar is a 1x1 km² average of the absolute difference in terms of dBZ for pulses at equal range separated by two pulses or 8 ms. This has been shown, when incorporated with a threshold on neighbouring maximum local gradients, to be an efficient method of ground clutter identification for incoherent radar. For the example given, the parameterisation eliminates all pixels with mean values of SIGMA < 3.5 dB and all surrounding pixels with maximum absolute horizontal gradients > 8 dBZ/km (relative to their eight closest pixels). This approach allows the identification of regions of anomalous propagation and has been shown to remove over 99% of regular ground clutter in dry conditions, while affecting less than 2% of precipitation measurements (Nicol et al., 2003).

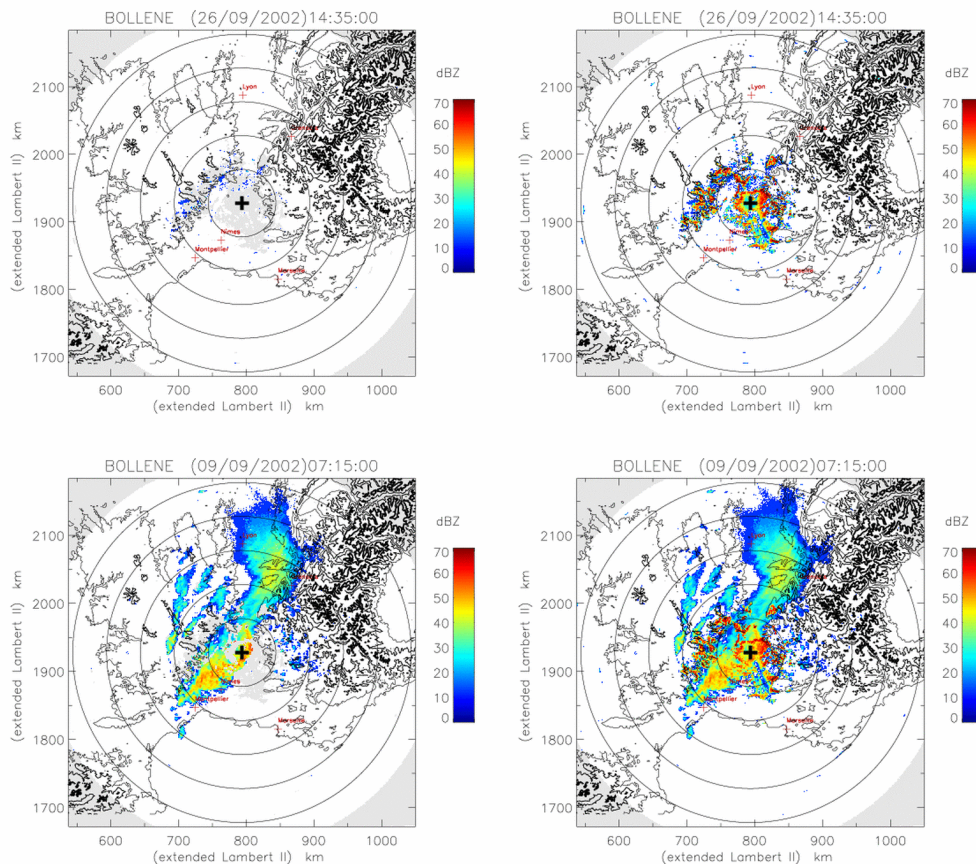


Figure 3: PPIs at 0.8° with clutter-processed data (left) and raw data (right) shown for a dry weather example (upper) and an example in precipitation (lower). The range rings correspond to 50 km.

Figure 3 shows examples of the clutter recognition procedure on images with and without rain. The upper plots show PPIs at an elevation of 0.8° (scan rate $10^\circ/\text{s}$) in non-raining, standard propagation conditions, both with (left) and without (right) clutter elimination. The lower plots show corresponding images for measurements at the same elevation in rain. Notice the ability to retain measurements in cluttered regions when the precipitation signal dominates.

Beam shielding

Shielding effects are currently corrected using VISHYDRO (Pellarin et al. 2002), which estimates the screening factors from a digital terrain model (DTM) and models of beam strength, propagation path and back-scattering coefficients. Long term accumulations conditioned on the occurrence of rain will be used to provide a complementary detection of screening effects, expected to be particularly useful with respect to anthropic targets. Accumulations will be analysed to identify regions showing marked discontinuities even when corrected, which may then be disregarded in radar estimates and may also be used to "fine-tune" the beam corrections applied.

Validation with rain gauges

There are 365 rain gauges providing daily accumulations in the research region. These measurements are used to create estimates of accumulated rain fields through krigage, utilising the estimated variogram of the gauge measurements. The gauge derived fields are then used in comparison with the radar estimated rain fields in two ways. Firstly, comparison is made for purposes of calibration adjustment. Secondly, comparisons are made to evaluate the degree of improvement gained by various correction procedures. In both cases, only regions of the kriged-gauge fields with a low estimated standard deviation (typically measurements near the gauge sites) and sufficient accumulations (in the examples given, std. dev. $< 40\%$ and accum. $> 5\text{ mm}$ are used). For the purpose of calibration, regions are also screened for shielding corrections ($< 1\text{ dB}$), for ground clutter in dry conditions ($< 8\text{ dBZ}$) and within limited ranges from the radar. Both, a minimum range (10 km) to avoid strong clutter interference and a maximum range (80 km) to reduce vertical profile effects, have been used. To evaluate the influence of various correction procedures, the screening criteria may be relaxed. For example, to evaluate the improvement obtained by a vertical profile correction procedure, the maximum range may be extended (e.g. 140 km) and comparisons made with and without correction.

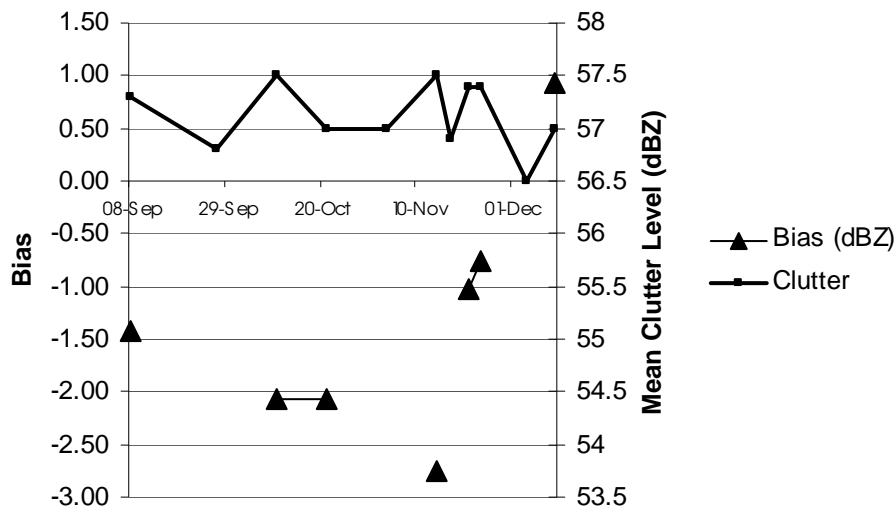


Figure 4: The calculated bias in rain accumulations for seven significant events near the radar region using the Z-R relationship with ($a=214$, $b=1.54$). Negative values indicate radar underestimation.

The criteria used to evaluate the comparison of rain accumulations are as follows (all criteria are calculated in terms of rain accumulation). The bias (ratio of averages which are used to calculate the radar calibration bias), the determination coefficient, that is, the square of the correlation coefficient (as a measure of the co-variation of the two estimated fields), the mean absolute fractional error and the Nash criterion (Nash and Sutcliffe, 1970). In this case, the Nash criterion is given in equation 1, where R_i are the gauge field estimates and R_i^{rad} are the corresponding radar rain field estimates over the selected regions. This criterion has the advantage that it is sensitive to both average differences (like the bias) and co-variation (like the

determination coefficient). Note that $N=1$ denotes perfect agreement while $N=0$ denotes estimates as poor as the average value as an estimate everywhere.

$$N = 1 - \frac{\sum_{i=1}^n (R_i - R_i^{rad})^2}{\sum_{i=1}^n (R_i - \frac{1}{n} \sum_{i=1}^n R_i)^2} \quad (1)$$

The bias in rainfall accumulations calculated for seven significant events (with maximum rain gauge accumulations ranging from 66 mm to 689 mm) are shown in Figure 4 as triangles. The radar estimated accumulations use a power-law Z-R relationship with the coefficients ($a=216$, $b=154$). The examples use areas ranging between from 500 km² and 4000 km² for the comparisons. In two situations, relatively closely spaced events (11 and 3 days apart) show nearly identical biases, possibly due to similar synoptic conditions (hence similar VPR and Z-R relationship effects). In general, significant variations in bias occur over a range of nearly 4 dB. It is intended to determine the relative importance of the VPR, Z-R relationship and radar stability on these differences.

Stability

The stability of the radar signal is tested using regions of high intensity and low variability at near range. These regions, while unlikely to be influenced by rainfall itself, may vary through surface wetting, providing difficulties in defining stable measurements. The idea is to detect drifts and sudden changes in the transmitted signal or receiver characteristics. The mean and median of regions of high intensity and low variability will be examined for this purpose. The median may prove more stable given that the number of pixels considered for stability may vary given the presence or otherwise of precipitation. Figure 4 shows the mean of the selected regions for each event corresponding to the accumulation biases also shown in Figure 4, along with several interspersed dry days. Here, the average dBZ is calculated over suitable pixels every 5 min. for the 0.8° elevation scan, then averaged over the event. The stability check regions are defined using thresholds of dBZ > 45, SIGMA < 2 and range < 40 km). As may be seen, the mean levels in dry conditions are typically around 0.5 dB less than during rain events. Additionally, the range of variation is approximately 1 dB with no clear relationship between the mean clutter levels and bias calculations. Further work is required on the robustness of the stability (clutter) estimates. However, assuming that the mean intense clutter levels overestimate changes in the radar stability due to independent changes (i.e. wetting and precipitation coverage), VPR and Z-R relationship effects would appear to be more dominant factors affecting accumulation biases.

Z-R relationship sensitivity

The estimates of radar reflectivity are converted to rainfall rate estimates using a standard power law Z-R relationship. The coefficients are derived from drop size distribution measurements previously made in the study region by Salles et al. (1999) for mixed synoptic conditions ($a=214$, $b=1.54$). A second relationship derived from the same study but for convective rainfall ($a=528$, $b=1.42$) is being tested for the improved estimation of rain accumulations. For three cases, the two relationships are applied and the overall calibration adjusted by the bias between radar and rain gauge estimates in regions of high accuracy for the two estimated rain fields. The examples shown in Table 1 involve the extreme event of 8-9th Sept. and two other significant events of 10th Oct. and 10th-12th Dec. This is hoped to indicate the benefit of distinct Z-R relationships in the context of event-long accumulations in a variety of conditions.

Table 1: Radar/Rain Gauge comparison criteria for three events after recalibration with gauge measurements for ($a=216, b=1.54$ and $a=528, b=1.42$ [bracketed]). Negative bias implies radar underestimation.

Event	Gauge Max (mm).	No. of pixels (1km ²)	Bias (dBZ)	Determination coefficient	Mean abs. fractional diff.	NASH criterion
8-9th Sept.	689	3983	-1.4 [-3.6]	0.91 [0.90]	0.18 [0.18]	0.90 [0.90]
10th Oct.	73	1719	-2.1 [-5.1]	0.57 [0.56]	0.21 [0.21]	0.47 [0.40]
10-12th Dec.	303	2259	0.9 [-2.3]	0.74 [0.72]	0.37 [0.42]	0.70 [0.59]

In general, after adjustment for calculated radar/gauge biases, similar values of the validation criteria are obtained for the two sets of Z-R coefficients. This is particularly the true for the intense convective event (8-

9th Sept.), where the spatial agreement between the radar and gauge measurements is excellent. There is a disparity of around 2.8 dB on average and 2.2 dB for this event, suggesting that the coefficient a in the convective Z-R relationship ($a=528$, $b=1.42$) should be rescaled to the range ($a=280-320$, $b=1.42$) to be consistent with the mixed Z-R coefficients ($a=216$, $b=1.54$) for a given radar calibration. The other events, which display distinctly different VPRs (as shown in the next section) show a slight preference for the mixed Z-R coefficients, based primarily on the Nash criteria. Globally, it seems that little benefit is gained with the convective Z-R relationship for event-long accumulations, although greater differences are likely to be found analysing hourly accumulations.

VPR observations

The analysis and correction of the vertical profile of reflectivity (VPR) is in the early stages, i.e. analysis. The first step involves the removal of ground clutter and the correction for beam shielding. After this, the profile for a certain region is calculated by averaging the reflectivity (Z) measurements weighted by the relative power distribution of the measurement at each altitude ($\Delta h = 200$ m) within the 3-dB beamwidth of the beam centre assuming a Gaussian distributed beam pattern. This is believed to produce more realistic and appropriately averaged estimates of the apparent vertical profile of reflectivity. The number of rain measurements and the percentage at each altitude relative to the possible number for a given averaging region is calculated to assure the quality of the measurements. Finally, all profiles must be continuous between the lowest measurement and 2 km.

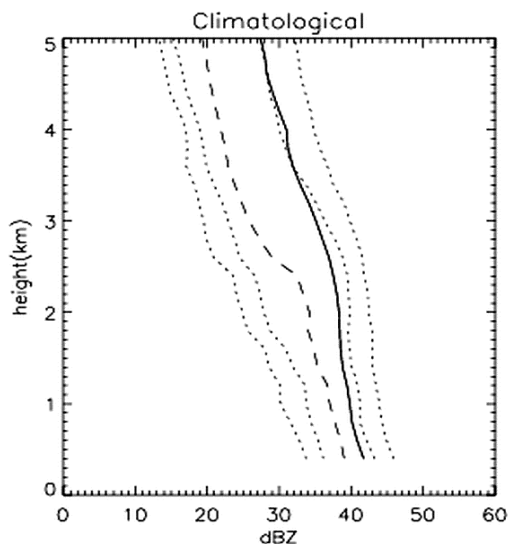


Figure 5: 'Climatological' VPR based on 626 sets of 10 min. volume scans during Bollene 2002. The mean profile is shown as a solid line and the 10%, 25%, 50%, 75% and 90% quantiles are shown as dashed lines.

The measurements for the 'climatological' VPR at each altitude are based on 626 profiles selected from ten events during the study period. These are averaged (solid line) and ranked as 10%, 25%, 50%, 75% and 90% quantiles (dashed lines), as shown in Figure 5. The following examples involve measurements from each 10 min. volume scan averaged in terms of reflectivity (Z) between 10 km and 40 km. This ensures a relatively narrow beamwidth though sufficient sampling up to 10 km altitude for analysis of deep convective systems for the scanning strategy employed. The profiles are shown between the altitudes of 600 m and 5 km relative to the radar (328 m ASL), over which the profiles are considered robust (based on the analysis of the number of estimates averaged at each height for each and the ensemble of the profiles). The climatological profiles show significant growth in reflectivity at all levels. On average there is a gradient of approximately -3 dB/km. The climatological profile shows a gradient with increasing height of around -4 dBZ/km at the altitudes between 2 km and 5 km. At altitudes below 2.5 km, the profile has values around -2 dBZ/km. Weaker profiles represented by the lower quantiles show a gradient of around -4 dBZ/km throughout the lower 5 km. More intense profiles show a gradient of around -4 dBZ/km between 2.5 km and 5 km, and a gradient of -1.5 dBZ/km below 2.5 km. In any case, radar estimates of rainfall would be expected to significantly underestimate rain accumulations at far range.

In Figure 6, examples are shown of significantly different vertical profiles of reflectivity between 600 m and 4 km for the three events presented in the previous section, again the altitude range has been selected for reasons of robustness. The first (8-9th Sept.) involves an example of deep convection, while the other two display characteristics of a strong bright band (10th Oct.) and very shallow rainfall with no or little bright band (10th-12th Dec.). The number of profiles derived from 10 min. volume scans are 176 (~29 hours), 23 (~4 hours) and 102 (17 hours) respectively for the events. The mean profile is shown as a solid line and the 10%, 25%, 50%, 75% and 90% quantiles are shown as dashed lines. The later two profiles show a very consistent profile structure throughout the events (up to 17 hours in one case). This suggests the great benefit of real-time VPR identification and correction relative to 'climatological' corrections for these events considering the significantly different structures of the profiles. The first case displays more variation in profile structure, while better typified by a mean decrease with altitude, though still somewhat in disparity with the climatological profiles shown in Figure 5. The more uniform behaviour of this profile in the lowest two kilometres may explain the significantly better agreement with gauge measurements after global adjustment (see Table 1).

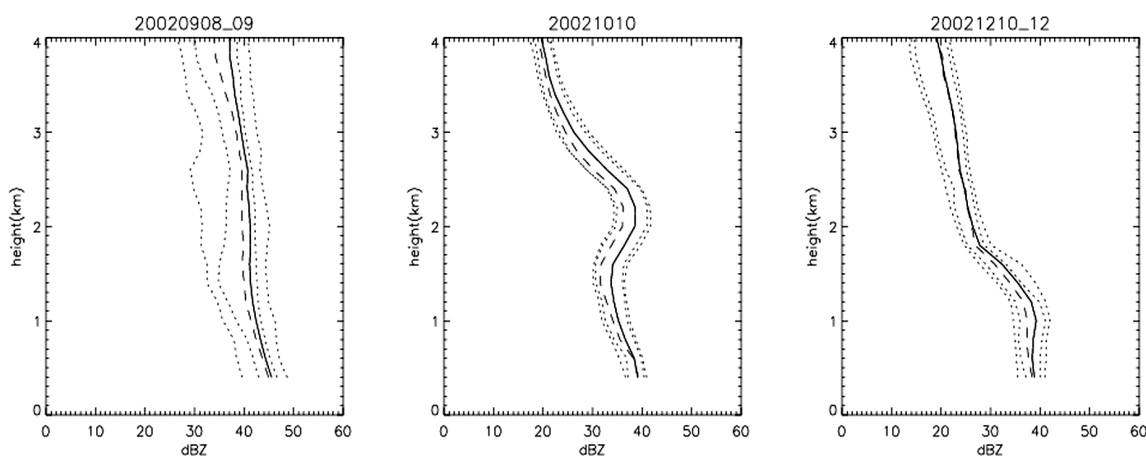


Figure 5: VPR for three events, 8-9th Sept., 10th Oct. and 10-12th Dec. (from left to right). The number of profiles derived from 10 min. volume scans are 176, 23 and 102 respectively for the events. The mean profile is shown as a solid line and the 10%, 25%, 50%, 75% and 90% quantiles are shown as dashed lines.

Correction procedures for the VPR will include the use of climatological and event-averaged profile as measured at near range and convolved with the beam width to mimic the influence of range. Profiles and corrections will also be investigated at event-scale and hourly time steps. Similarly, lesser spatial averaging will be examined to determine the optimal balance between robustness and resolution. It is previewed that the identification and allowance for the bright band is a primary consideration though the vertical gradients observed (both at altitude and in the lower layers) suggest that their accurate identification is also critical for accurate estimates of rain at ground level in this region.

Perspectives

In addition to the work mentioned previously, precipitation type identification is being implemented using the algorithms of Steiner et al (1995) using horizontal gradients for the detection of convective regions and of Sanchez-Diezma et al. (2000) for the identification of the bright band and hence regions of stratiform precipitation. VPR identification/correction along with specific Z-R relationships may then be applied for each rain type. There is certainly a need for the identification of the presence of a bright band, to correct for or avoid its influence and to distinguish a level for snowfall Z-R relationships.

Bollène 2003+

The success of Bollène 2002 has led to its expansion into 2003 and beyond with a second S-band radar (at Nimès), located only 60 km from the Bollène radar site, to be also operated over four months in the autumn 2003 in a volume scanning mode. The two radar will allow unprecedented comparisons of observed VPRs at different ranges and of the relative performance of precipitation type discrimination in this region. Additionally, two disdrometers are to be deployed in the study region throughout these periods, allowing the

determination of precipitation type independently from the radar and the calculation of suitable Z-R relationships.

Conclusions

The use of volume scanning strategies offer potential improvement to quantitative precipitation measurements in several ways. The availability of a larger number of measurements at a given site allows ground clutter sites to be disregarded and values interpolated from either above or neighbouring locations, this removes the incentive to partially filter cluttered data. Similarly with shielded data, while in this case, the measurements may be corrected using a digital terrain model, if sufficiently accurate corrections can not be proven, the measurements may again be disregarded and interpolation from other regions used.

Potentially the greatest benefits will be gained from the wealth of information on the vertical structure of reflectivity. Many, different profiles have been observed over the several months of data collection. One common trend, is the large degree of enhancement observed in the lower layers. Based on the shape of many of these profiles and the sampling height of the radar with range, the application of a VPR correction must greatly improve the accuracy of radar measurements with range.

While the selection of Z-R relationship does not seem to have a large bearing on the estimates of rainfall at the event scale, the identification of specific regions as convective, stratiform or transition may prove useful in applying these relationships especially at higher time scales.

References

Riverain, J. C. (1998). "Les episodes orageux à precipitations extrêmes dans les régions méditerranéennes du sud de la France". Phénomènes remarquables, no. 4, Météo France, SCEM, 1998, 93 pp.

Nash, J. E. & Sutcliffe, J. V. (1970). "River flow forecasting through conceptual models 1 A discussion of principles". *J. Hydrol.* **10**, 282-290.

Nicol, J. C., Tabary, P., Sugier, J., Parent-du-Chatelet, J. & Delrieu, G. (2003). "Non-weather echo identification for conventional operational radar". *Proceedings of the 31st Conference on Radar Meteorology*, AMS, Seattle, 542-545.

Salles, C., Sempere-Torres, D., & Creutin, J. D. (1999). "Characterisation of raindrop size distribution in Mediterranean climates: analysis of the variations on the Z-R relationship". *Proceedings of the 29th Conference on Radar Meteorology*, AMS, Montreal, 670-673.

Sánchez-Diezma, R., Zawadzki, I. & Sempere-Torres, D. (2000). "Identification of the bright band through the analysis of volumetric data". *J. Geophys. Res.* **105**(D2), 2225-2236.

Steiner, M., Houze, R. A. and Yuter, S. E. (1995). "Climatological characterisation of three-dimensional storm structure from operational radar and rain gauge data". *J. Appl. Meteor.* **34**, 1978-2007.